Model-guided identification of a therapeutic strategy to reduce hyperammonemia in liver diseases

Ahmed Ghallab, Geraldine Celliere, Sebastian Henkel, Dominik Driesch, Stefan Hoehme, Ute Hofmann, Sebastian Zellmer, Patricio Godoy, Agapios Sachinidis, Meinolf Blaszkewicz, et al.

AUTHOR QUERY FORM

ELSEVIER	**Journal: JHEPAT** **Article Number: 5901**	**Please e-mail your responses and any corrections to:** **E-mail: proofcorrections.esnl@elsevier.sps.co.in**

Dear Author,

Please check your proof carefully and mark all corrections at the appropriate place in the proof (e.g., by using on-screen annotation in the PDF file) or compile them in a separate list. Note: if you opt to annotate the file with software other than Adobe Reader then please also highlight the appropriate place in the PDF file. To ensure fast publication of your paper please return your corrections within 48 hours.

For correction or revision of any artwork, please consult http://www.elsevier.com/artworkinstructions.

Any queries or remarks that have arisen during the processing of your manuscript are listed below and highlighted by flags in the proof. Click on the 'Q' link to go to the location in the proof.

Location in article	Query / Remark: click on the Q link to go Please insert your reply or correction at the corresponding line in the proof
Q1	Your article is registered as a regular item and is being processed for inclusion in a regular issue of the journal. If this is NOT correct and your article belongs to a Special Issue/Collection please contact j.bakker@elsevier.com immediately prior to returning your corrections.
Q2	The author names have been tagged as given names and surnames (surnames are highlighted in teal color). Please confirm if they have been identified correctly.
Q3	The country name has been inserted for the affiliation `6'. Please check, and correct if necessary.
Q4	The affiliations `7' and `11' were identical, the latter has been removed, and hence the affiliation link the author `Rolf Gebhardt' has been changed, accordingly. Please check, and correct if necessary.
Q5	One or more sponsor names may have been edited to a standard format that enables better searching and identification of your article. Please check and correct if necessary.
Q6	The country names of the Grant Sponsors are provided below. Please check and correct if necessary. `BMBF' - `Germany'.

Please check this box if you have no corrections to make to the PDF file ☐

Thank you for your assistance.

Graphical abstract

Model-guided identification of a therapeutic strategy to reduce hyperammonemia in liver diseases pp xxx–xxx

Ahmed Ghallab *, Géraldine Cellière, Sebastian G. Henkel, Dominik Driesch, Stefan Hoehme, Ute Hofmann, Sebastian Zellmer, Patricio Godoy, Agapios Sachinidis, Meinolf Blaszkewicz, Raymond Reif, Rosemarie Marchan, Lars Kuepfer, Dieter Häussinger, Dirk Drasdo, Rolf Gebhardt, Jan G. Hengstler *

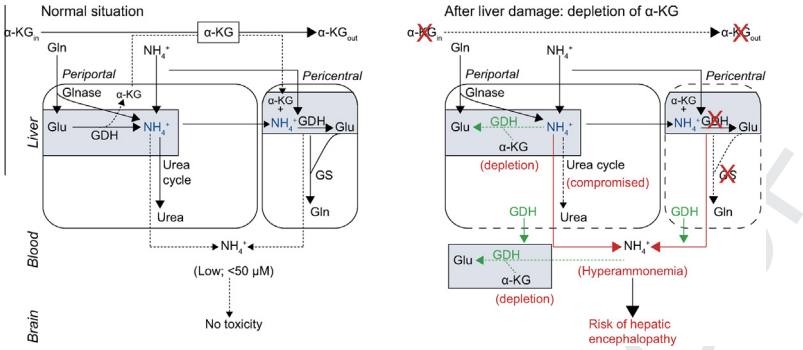

Research Article

EASL JOURNAL OF HEPATOLOGY

Model-guided identification of a therapeutic strategy to reduce hyperammonemia in liver diseases

Ahmed Ghallab[1,2,*], Géraldine Cellière[3,†], Sebastian G. Henkel[4,†], Dominik Driesch[4], Stefan Hoehme[5], Ute Hofmann[6], Sebastian Zellmer[7], Patricio Godoy[1], Agapios Sachinidis[8], Meinolf Blaszkewicz[1], Raymond Reif[1], Rosemarie Marchan[1], Lars Kuepfer[9], Dieter Häussinger[10], Dirk Drasdo[3,5,‡], Rolf Gebhardt[7,‡], Jan G. Hengstler[1,*,‡]

[1]*Leibniz Research Centre for Working Environment and Human Factors at the Technical University Dortmund, Dortmund, Germany;* [2]*Department of Forensic Medicine and Toxicology, Faculty of Veterinary Medicine, South Valley University, Qena, Egypt;* [3]*Institute National de Recherche en Informatique et en Automatique (INRIA), INRIA Paris-Rocquencourt & Sorbonne Universités UPMC Univ Paris 6, LJLL, France* [4]*BioControl Jena GmbH, Jena, Germany;* [5]*Interdisciplinary Centre for Bioinformatics, University of Leipzig, Leipzig, Germany;* [6]*Dr. Margarete Fischer-Bosch Institute of Clinical Pharmacology and University of Tuebingen, Germany;* [7]*Institute of Biochemistry, Faculty of Medicine, University of Leipzig, Leipzig, Germany;* [8]*Institute of Neurophysiology and Center for Molecular Medicine Cologne (CMMC), University of Cologne, Robert-Koch-Str. 39, 50931 Cologne, Germany;* [9]*Computational Systems Biology, Bayer Technology Services GmbH, Leverkusen, Germany;* [10]*Clinic for Gastroenterology, Hepatology and Infectious Diseases, Heinrich-Heine-University, Düsseldorf, Germany*

Background & Aims: Recently, spatial-temporal/metabolic mathematical models have been established that allow the simulation of metabolic processes in tissues. We applied these models to decipher ammonia detoxification mechanisms in the liver.
Methods: An integrated metabolic-spatial-temporal model was used to generate hypotheses of ammonia metabolism. Predicted mechanisms were validated using time-resolved analyses of nitrogen metabolism, activity analyses, immunostaining and gene expression after induction of liver damage in mice. Moreover, blood from the portal vein, liver vein and mixed venous blood was analyzed in a time dependent manner.
Results: Modeling revealed an underestimation of ammonia consumption after liver damage when only the currently established mechanisms of ammonia detoxification were simulated. By iterative cycles of modeling and experiments, the reductive amidation of alpha-ketoglutarate (α-KG) via glutamate dehydrogenase (GDH) was identified as the lacking component. GDH is released from damaged hepatocytes into the blood where it consumes ammonia to generate glutamate, thereby providing systemic protection against hyperammonemia. This mechanism was exploited therapeutically in a mouse model of hyperammonemia by injecting GDH together with optimized doses of cofactors. Intravenous injection of GDH (720 U/kg), α-KG (280 mg/kg) and NADPH (180 mg/kg) reduced the elevated blood ammonia concentrations (>200 μM) to levels close to normal within only 15 min.
Conclusion: If successfully translated to patients the GDH-based therapy might provide a less aggressive therapeutic alternative for patients with severe hyperammonemia.

Keywords: Systems biology; Spatio-temporal model; Ammonia; Liver damage; Liver regeneration.
Received 23 March 2015; received in revised form 15 November 2015; accepted 16 November 2015

* Corresponding authors. Addresses: Leibniz Research Centre for Working Environment and Human Factors, IfADo – Ardeystr. 67, D-44139 Dortmund, Germany. Tel.: +49 02311084 356; fax: +49 02311084 403 (A. Ghallab) or Leibniz Research Centre for Working Environment and Human Factors, IfADo – Ardeystr. 67, D-44139 Dortmund, Germany. Tel.: +49 02311084 349; fax: +49 02311084 403 (J.G. Hengstler).
E-mail addresses: ghallab@ifado.de (A. Ghallab), hengstler@ifado.de (J.G. Hengstler).
† These authors contributed equally to the work.
‡ These authors share co-senior authorship.

Abbreviations: CCl_4, carbon tetrachloride; GDH, glutamate dehydrogenase; AOA, aminooxy acetate; ALT, alanine transaminase; AST, aspartate transaminase; α-KG, alpha-ketoglutarate; PDAC, 2,6-pyridinedicarboxylic acid.

Introduction

Recent developments have strongly improved our capability to generate information at multiple spatial and temporal scales [1,2]. However, research on disease pathogenesis is hampered by the difficulty to understand the orchestration of individual components. Here, mathematical models help to formalize relations between components, simulate their interplay, and to study processes that are too complex to be understood intuitively [1]. This is particularly important when studying the pathophysiology of metabolic liver diseases, where due to zonation different metabolic processes take place in pericentral and periportal hepatocytes [3]. To be able to investigate such complex processes we recently established a technique of integrated metabolic spatial-temporal modeling (IM) [4]. These IM integrate conventional metabolic models into spatial-temporal models of the liver lobule [1,4,5]. The present study was motivated by the IM predictions, which proposed that the conventional mechanisms where ammonia is metabolized by urea cycle enzymes in the periportal compartments of the liver lobules and by glutamine synthetase (GS) reaction in the pericentral compartments (Supplementary

Please cite this article in press as: Ghallab A et al. Model-guided identification of a therapeutic strategy to reduce hyperammonemia in liver diseases. J Hepatol (2016), http://dx.doi.org/10.1016/j.jhep.2015.11.018

Research Article

Fig. 1) failed to explain the experimental findings [4]. The IM was applied to an experimental scenario, where the entire pericentral and a part of the periportal compartment of the liver lobules were destroyed by a single high dose of the hepatotoxic compound carbon tetrachloride (CCl_4). This leads to compromised nitrogen metabolism and hyperammonemia. In the present study, we performed a series of new experiments accompanied by simulations with novel models to explore the mechanism responsible for the observed discrepancy. Experimentally, the time-resolved analysis of metabolites and metabolic activities after CCl_4 intoxication offers good conditions to study ammonia detoxification and possible compensatory mechanisms during the damage and regeneration process. Time-resolved analysis of metabolites was performed in the portal vein and heart blood, representing the 'liver inflow', and in the liver vein as 'liver outflow'. These analyses allowed a precise experimental validation of model predictions. Finally, iterative cycles of modeling and experimental validation allowed the identification of a so far unrecognized mechanism of ammonia detoxification. Importantly, this mechanism could be exploited therapeutically to reduce elevated blood ammonia concentrations close to normal levels by intravenous injection of glutamate dehydrogenase (GDH; 720 U/kg) and its cofactors alpha-ketoglutarate (α-KG; 280 mg/kg) as well as NADPH (180 mg/kg). This example illustrates how concrete therapies can be derived by model guided experimental strategies.

Liver Failure and Growth

Materials and methods

A detailed description of materials and methods is provided in the Supplementary materials. Male C57BL/6N 10–12 weeks old mice were used (Charles River, Sulzfeld, Germany). Acute liver damage was induced by intraperitoneal injection of 1.6 g/kg CCl_4, unless other doses are indicated. Blood was taken from mice under anesthesia from the portal and hepatic veins, as well as the right heart chamber, and plasma was separated. Liver tissue samples were collected from defined anatomical positions for histopathology, immunohistochemistry, enzyme activity assays, gene array and q-RT-PCR analyses. The dead cell area was quantified in hematoxylin and eosin stained tissue sections using Cell^M software (Olympus, Hamburg, Germany). Whole-genome analysis of gene expression in mouse liver tissue was performed in control as well as after CCl_4 intoxication with Affymetrix gene arrays. The latter techniques are described fully in the Supplementary materials and methods. The analysis of ammonia and further metabolites was performed using commercially available kits. Concentrations of amino acids and organic acids in liver tissue were measured in duplicate using GC-MS. GS, GDH and transaminases activity assays were performed photometrically as described in the Supplementary materials and methods. $NADP^+$ and NADPH were analyzed by LC-MS. Mouse hepatocytes were isolated by a two-step EGTA/collagenase perfusion technique and either used directly in suspension or cultivated in collagen sandwiches (Supplementary materials and methods). For the mathematical modeling of ammonia and the related metabolites the integrated metabolic, spatio-temporal model was applied [4,5]. In addition, the IM was replaced by a set of novel models that include further reactions and the blood compartment of the liver (Supplementary materials and methods). Statistical analysis was done with SPSS software as described in the Supplementary materials.

Results

An integrated spatial-temporal-metabolic model suggests a so far unrecognized mechanism of ammonia detoxification

The detoxification process in healthy, damaged and regenerating livers was simulated using a recently established integrated metabolic IM [4]. To compare the simulated metabolite concentrations with the *in vivo* situation, an experiment was performed in which blood was collected from the portal vein (representing 85% of the 'liver inflow'), the heart (representing 15% of the 'liver inflow'), and the hepatic vein (representing the 'liver outflow') in a time-resolved manner after CCl_4 injection (Fig. 1A; Supplementary Fig. 2). The result shows that ammonia is detoxified during its passage through the liver as illustrated by the difference in ammonia concentrations between the portal vein and the hepatic vein in the control mice (Fig. 1B). This detoxification process is compromised after liver damage, particularly on days 1 and 2. Surprisingly, the IM model predicted higher ammonia concentrations than those experimentally observed, particularly on day 1 (Fig. 1C; see the video in the Supplementary data). Analyses of heart blood demonstrate the contribution of the extrahepatic compartment, which includes brain, muscles, kidneys and blood, to ammonia detoxification between days 1 and 4 after the induction of liver damage. However, this extrahepatic contribution is small compared to detoxification by the liver (Supplementary Figs. 2–8). In addition to the time-resolved study, similar experiments were also performed in a dose dependent manner on day 1 after CCl_4 administration when the discrepancy between simulated and measured ammonia was maximal. For this purpose, doses ranging between 10.9 and 1600 mg/kg CCl_4 were tested, resulting in a concentration dependent increase in the dead cell area, with only the highest dose causing damage to the entire CYP2E1 positive pericentral region of the liver lobule (Fig. 1D; Supplementary Fig. 9A, B). Destruction of the GS positive area occurred in with doses ranging between 38.1 and 132.4 mg/kg (Fig. 1D, E; Supplementary Fig. 9C); also *CPS1* showed a dose dependent decrease (Supplementary Fig. 9C) leading to compromised ammonia metabolism (Supplementary Fig. 10). Using the IM [4], we also observed a discrepancy between the predicted and measured ammonia in the dose dependent study (Fig. 1F).

To find an explanation for this discrepancy, we performed time-resolved gene array analysis of mouse liver tissue after CCl_4 intoxication (Fig. 2A). Fuzzy clustering identified seven gene clusters which reflected time dependent gene expression alterations [6]. Clusters 4 and 6 contained genes whose expression was transiently repressed at early time points after CCl_4 intoxication (Fig. 2B). Further bioinformatics analyses revealed an over representation of nitrogen/ammonia metabolism KEGG and Gene ontology terms of genes in cluster 4 (Fig. 2C, D). Genes relevant for ammonia metabolism were further studied by qRT-PCR, immunostaining and activity assays. GS is the key enzyme for ammonia detoxification in the pericentral compartment. RNA levels of GS started to decrease as early as 6 h after CCl_4 injection, it was at its lowest between days 1 and 4, before finally recovering to initial levels between days 6 and 30 (Fig. 2E). A similar time-dependent curve was obtained for GS activity although the decrease occurred slightly later than that of RNA with very low levels between days 2 and 4 (Fig. 2E). The pattern and intensity of GS immunostaining was found to be comparable to GS activity (Fig. 2F). In addition, ornithine aminotransferase (OAT), an enzyme exclusively localized in GS positive pericentral hepatocytes that provides additional glutamate for fixing ammonia [7], decreased to almost undetectable levels with a delayed recovery (Supplementary Fig. 3A). The key enzymes of the periportal compartment, CPS1, ASS1, ASL and arginase1 were similarly analyzed in the same tissue (Supplementary Figs. 3B and 4). Extending the IM [4], with time-dependent

Please cite this article in press as: Ghallab A et al. Model-guided identification of a therapeutic strategy to reduce hyperammonemia in liver diseases. J Hepatol (2016), http://dx.doi.org/10.1016/j.jhep.2015.11.018

JOURNAL OF HEPATOLOGY

enzyme concentrations (model 1), did not remove the discrepancy between model predictions and experimental data (Supplementary Fig. 11), indicating that our model lacks a relevant, but so far unrecognized mechanism of ammonia detoxification.

Acute liver damage provides systemic protection against ammonia by GDH release

Further evidence that an unrecognized mechanism of ammonia detoxification exists arose from metabolic analyses performed

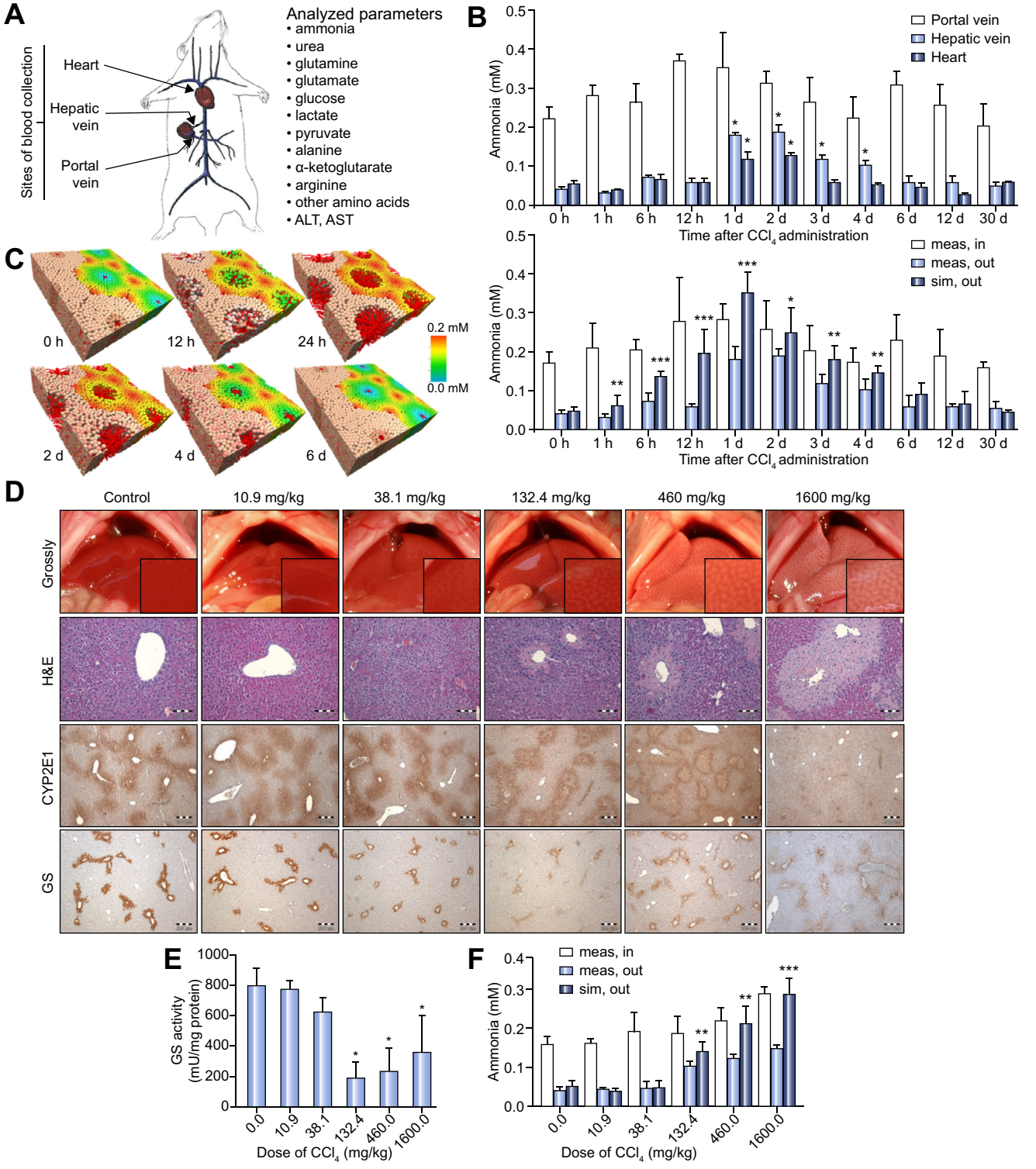

Please cite this article in press as: Ghallab A et al. Model-guided identification of a therapeutic strategy to reduce hyperammonemia in liver diseases. J Hepatol (2016), http://dx.doi.org/10.1016/j.jhep.2015.11.018

Research Article

using plasma from mice after CCl_4 injection (Fig. 3A). Most of the analyzed factors in plasma (urea, glutamine, glucose, lactate, pyruvate, alanine, arginine and other amino acids: Supplementary Figs. 4–6) were within the expected concentration ranges, α-KG, which dramatically decreased between 12 h and day 2 (Fig. 3A). This decrease was accompanied by an almost concurrent increase in glutamate levels, which persisted longer than the drop in α-KG. One potential explanation is the delayed recovery of GS, which uses glutamate and ammonia to form glutamine (Fig. 2E, F). The decrease in α-KG (and the increase in glutamate) was also accompanied by increased GDH activity in plasma, because GDH is released from damaged hepatocytes (Fig. 3A). The present observations suggest that GDH released from the damaged hepatocytes into the blood catalyzes, at least transiently, a reaction that consumes ammonia to produce glutamate (Fig. 3D). To test this hypothesis, we collected plasma from mice on day 1 after CCl_4 injection. Addition of α-KG alone was sufficient to slightly but significantly decrease blood ammonia concentrations (Fig. 3B). This decrease was enhanced by further adding NADPH and particularly GDH; whereas the GDH inhibitor, PDAC completely antagonized the effect. To test also higher ammonia concentrations typically observed in patients with severe pre-coma hyperammonemia, 600 μM ammonia was added to plasma collected on day 1 after CCl_4 administration. Under these conditions, α-KG also reduced ammonia and increased glutamate concentrations (Fig. 3C; Supplementary Fig. 12A). Together, these experiments suggest that a GDH reaction consuming ammonia in blood takes place when GDH is released from acutely damaged livers (Fig. 3D).

Validation of the 'GDH-driven ammonia consumption' in hepatocytes

The experiments described above suggest that high ammonia concentrations in plasma leads to a 'reverse' GDH reaction, which consumes rather than produces ammonia. To test whether this 'GDH-driven ammonia consumption' occurs not only in plasma but also in cells, we used an *in vitro* system with primary mouse hepatocytes incubated with ammonia in suspension (Fig. 4). PDAC was used to inhibit GDH (Fig. 4A) in order to determine its influence on ammonia metabolism. In hepatocytes isolated from control mice, unphysiologically high ammonia concentrations (2 mM) were required until PDAC caused a significant increase of ammonia levels in the suspension buffer (Fig. 4B). However, when hepatocytes from mice 24 h after CCl_4 intoxication were used, PDAC treatment increased ammonia concentrations in the suspension buffer, even with 0.5 mM ammonia. Furthermore, in the absence of ammonia, hepatocytes secreted a small but statistically significant amount of ammonia into the buffer. Similarly, glutamate production was reduced by PDAC, an effect that was also stronger in hepatocytes isolated from CCl_4-exposed mice (Fig. 4C), which corresponds to the reverse GDH reaction proposed in Fig. 3D (right panel). CCl_4 destroys the pericentral hepatocytes (Fig. 1D), which explains the reduced glutamine generation by GS (Fig. 4D) and compromises urea cycle enzymes (Supplementary Fig. 3B, C), which explains the reduced urea production (Fig. 4E). Similar experiments were also performed with cultivated (instead of suspended) hepatocytes from untreated mice. The results demonstrate that inhibition of GDH at high ammonia concentrations increases ammonia-induced cytotoxicity (Supplementary Fig. 12B). These results show that the catalytic direction of GDH reverses a clearly becomes ammonia consuming also in hepatocytes in order to compensate the compromised metabolism by urea cycle enzymes and GS after intoxication.

Further evidence emerges from simulations with a set of novel models 1–4 (Supplementary Fig. 11). If a reversible GDH reaction was integrated into the hepatocyte compartment (Fig. 5A; Supplementary Fig. 11), the discrepancy between *in vivo* measured and simulated ammonia concentrations (Fig. 1C) completely disappeared (Fig. 5B). The quantitative agreement was obtained even without considering the blood compartment of the liver, suggesting that after CCl_4-induced damage, the ammonia consumption catalyzed by GDH in the hepatocytes represents the missing ammonia sink predicted by [4].

Therapy of hyperammonemia based on the reverse GDH reaction

The above described ammonia consumption catalyzed by the GDH reaction (Figs. 3B–D and 4) and the aforementioned decrease in plasma α-KG levels (Fig. 3A) prompted us to test whether supplementation of α-KG in mice helps to detoxify ammonia. Therefore, mice received a hepatotoxic dose of CCl_4 (1.6 g/kg) and 24 h later α-KG (280 mg/kg) was injected into the tail vein. Blood was collected immediately before as well as 15, 30 and 60 min after injection of α-KG. A decrease in plasma ammonia concentrations by 31, 40 and 43% was observed 15, 30 and 60 min after α-KG injection, respectively (Fig. 6A). Glutamate increased after 15 min and decreased again after longer periods probably due to the consumption by further metabolism. α-KG transiently increased in plasma after injection and then rapidly decreased. Analysis of GDH activity demonstrated that the experiment was performed under conditions of high plasma activity. In control mice, injection of α-KG did not alter blood concentrations of ammonia or glutamate (Fig. 6B). In addition, plasma α-KG levels were lower in CCl_4-treated mice compared to the control mice, suggesting increased consumption in mice with damaged livers.

Fig. 1. Evidence for a so far unrecognized mechanism of ammonia detoxification. (A) Experimental design. (B) Ammonia concentrations in the portal vein, hepatic vein and heart. $^{*}p$ <0.05 compared to the corresponding controls (0 h). (C) Integrated metabolic spatio-temporal model using the technique described by [4] (video in the Supplementary data). Predicted ammonia concentrations in the liver outflow are higher compared to the experimental data. $^{***}p$ <0.001, $^{**}p$ <0.01 and $^{*}p$ <0.05 compared to the measured ammonia output. (D) Dose dependent experiment (10.9 to 1600 mg/kg CCl_4 24 h after administration) showing macroscopic alterations with a spotted pattern at 132.4 mg/kg and higher doses, corresponding to the central necrotic lesion in hematoxylin/eosin staining, scale bars: 100 μm. Destruction of the pericentral CYP2E1 positive region which begins at 132.4 mg/kg with central necrosis still surrounded by CYP2E1 positive surviving hepatocytes; the entire CYP2E1 positive region was destroyed at the highest dose of 1600 mg/kg. The GS positive region was destroyed only at 132.4 mg/kg and higher doses, which corresponds to the decrease in GS activity (E), scale bars: 200 μm. $^{*}p$ <0.05 when compared to the control group (0). (F) Comparison of analyzed and simulated ammonia concentrations in the liver vein for the experiment in (D); meas, in: analyzed concentrations in the portal vein (representing 85% of the liver inflow) and heart blood (representing 15% of the liver inflow); meas. out: analyzed concentrations in the liver vein; sim. out: simulated concentrations in the liver vein. Data are mean values and SD of three mice per time point and dose of CCl_4. $^{***}p$ <0.001 and $^{**}p$ <0.01 compared to the measured ammonia output.

Please cite this article in press as: Ghallab A et al. Model-guided identification of a therapeutic strategy to reduce hyperammonemia in liver diseases. J Hepatol (2016), http://dx.doi.org/10.1016/j.jhep.2015.11.018

JOURNAL OF HEPATOLOGY

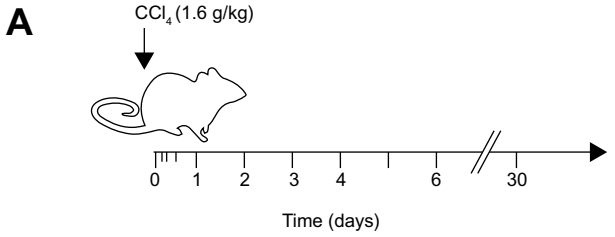

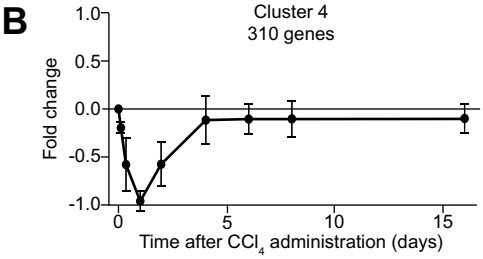

C

KEGG nitrogen metabolism		Time after CCl_4 administration								
Symbol	Name	Healthy liver	Hour 2	Hour 8	Day1	Day 2	Day 4	Day 6	Day 8	Day 16
Car1	Carbonic anhydrase 1	1	-1.12	-1.78	-2.42	-1.85	-1.11	1.1	1.15	1.02
Car3	Carbonic anhydrase 3	1	-2.94	-4.51	-32.55	-4.47	-1.33	-1.74	-1.71	-1.41
Car5a	Carbonic anhydrase 5a, mitochondrial	1	-1.64	-4	-4.44	-1.96	1.1	-1.17	1.02	-1.1
Cth	Cystathionase (cystathionine γ-lyase)	1	-1.28	-1.95	-2.59	-2.03	1.35	-1.08	-1.04	-1.09
Gls2	Glutaminase 2 (liver, mitochondrial)	1	-1.65	-2.44	-3.71	-2.13	-1.06	-1.26	-1.01	-1.14
Glul	Glutamate-ammonia ligase (glutamine synthetase)	1	1.13	-1.84	-5.82	-4.85	-2.36	-1.02	-1.27	-1.08
Hal	Histidine ammonia lyase	1	-1.71	-3.09	-3.86	-2.11	1.05	-1.37	1.14	1

D

GO urea cycle/urea metab. process		Time after CCl_4 administration								
Symbol	Name	Healthy liver	Hour 2	Hour 8	Day 1	Day 2	Day 4	Day 6	Day 8	Day 16
Aldh6a1	Aldehyde dehydrogenase family 6, subfamily A1	1	-1.15	-1.63	-2.33	-2.09	-1.24	1.02	1.02	-1.03
Dpyd	Dihydropyrimidine dehydrogenase	1	-1.28	-1.71	-2.63	-2.15	-1.27	-1.08	1.07	-1.02
Dpys	Dihydropyrimidinase	1	-1.26	-2.91	-3.35	-1.87	-1.08	-1.01	-1.05	-1.12
Asl	Argininosuccinate lyase	1	1.06	1.5	-2.12	-1.74	-1.13	-1.13	-1.05	-1.09
Cebpa	CCAAT/enhancer binding protein (C/EBP), alpha	1	-1.25	-1.35	-2.07	-1.4	1.06	1.14	1.05	-1.07
Otc	Ornithine transcarbamylase	1	-1.22	-1.89	-3.26	-2.14	1.06	-1.08	1.01	-1.01

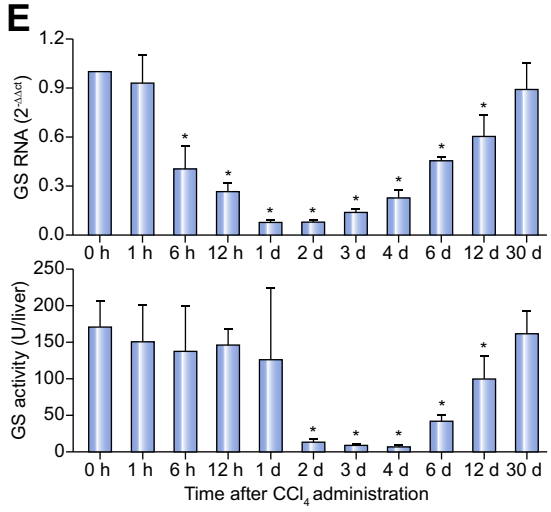

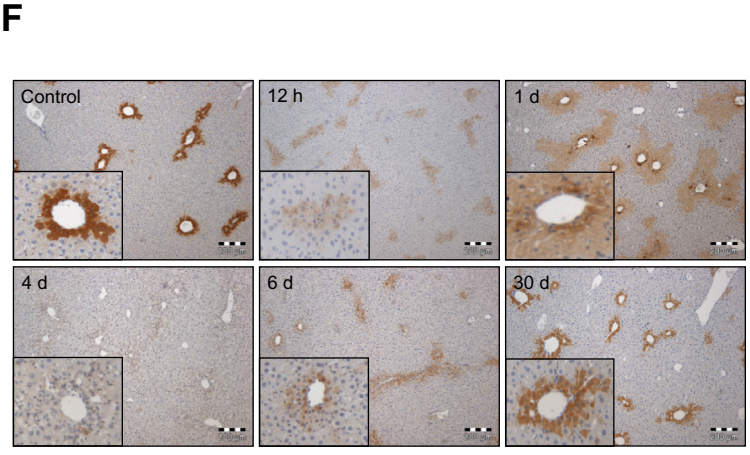

Fig. 2. Spatio-temporal alterations of ammonia metabolizing enzymes after CCl_4 intoxication. (A) Experimental design. (B) Time dependent changes of gene expression in fuzzy cluster 4 from [6]. The dots correspond to the average of the mean scaled values for all 310 genes, between their respective maximal and minimal expression levels at each time point, using healthy liver (time 0) as reference. Error bars indicate standard error. (C) Changes in expression of genes associated to the KEGG terms ammonia/nitrogen metabolism (Gene Ontology [GO] ID 910) as revealed by KEGG pathways enrichment analysis in fuzzy cluster 4 ($p = 2.36 \times 10^{-7}$). (D) Changes in the expression of genes associated to the GO terms 'urea cycle/urea metabolic process' (Gene Ontology ID 0000050 and 0019627 respectively) as revealed by GO enrichment analysis in fuzzy cluster 4 ($p = 3.83 \times 10^{-4}$). In C and D, the values indicate fold of expression over healthy liver at each time point after CCl_4 administration, and correspond to the average of 5 independent biological replicates. Time course of GS RNA levels, GS activity (E) and immunostaining (F), Scale bars: 200 μm. $^*p$ <0.05 when compared to the control group (0 h).

Please cite this article in press as: Ghallab A et al. Model-guided identification of a therapeutic strategy to reduce hyperammonemia in liver diseases. J Hepatol (2016), http://dx.doi.org/10.1016/j.jhep.2015.11.018

Research Article

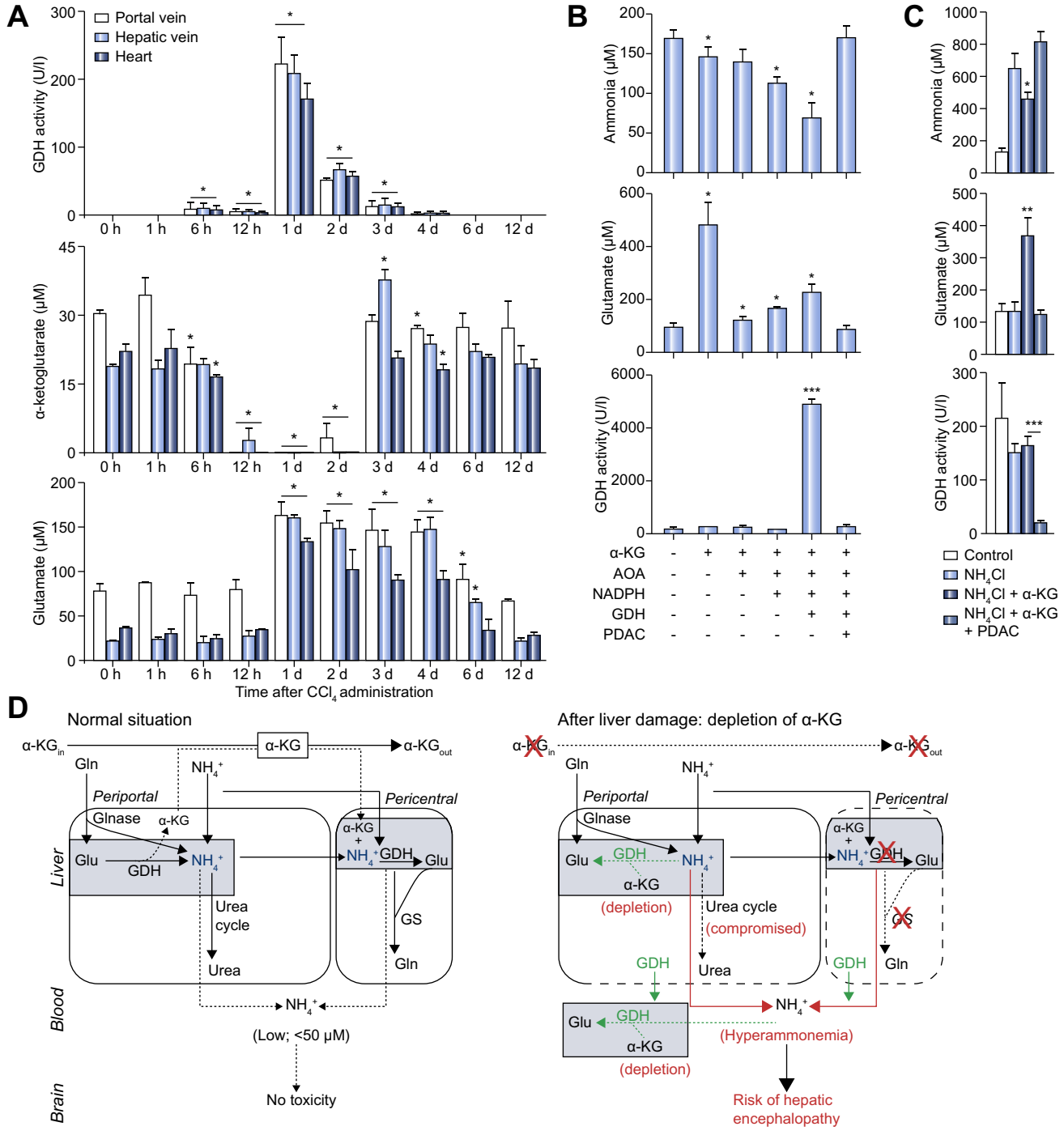

Fig. 3. Detoxification of ammonia by a reverse GDH reaction. (A) After induction of liver damage by CCl_4, plasma activity of GDH transiently increases. This is accompanied by a decrease in alpha-ketoglutarate (α-KG) and an increase in glutamate. $^{*}p$ <0.05 when compared to the corresponding control (0 h). Similar results were observed in liver tissue (Supplementary Tables 1 and 2). (B) Validation of the reverse GDH reaction using an inhibitor of GDH (PDAC). Plasma of mice 24 h after CCl_4 injection was analyzed. α-KG was added alone or in combination with AOA, NADPH, GDH and PDAC. $^{***}p$ <0.001, $^{**}p$ <0.01 and $^{*}p$ <0.05 when compared to controls (0). (C) A similar experimental design was chosen as in B. However, 600 μM ammonia was added to also test the reaction at a higher but still clinically relevant concentration. α-KG decreases ammonia and increases glutamate concentrations, which can be blocked by the GDH inhibitor, PDAC. $^{***}p$ <0.001, $^{**}p$ <0.01 and $^{*}p$ <0.05 when compared to the NH_4Cl group (0 h). Data are mean values and SD of 3 biological replicas. (D) Concept of the reverse glutamate dehydrogenase (GDH) reaction. In normal periportal hepatocytes, GDH generates ammonia, which is detoxified by the urea cycle. In pericentral hepatocytes, GDH generates glutamate which is required as a substrate for the GS reaction to form glutamine (Gln). Biosynthesis of α-KG takes place in the periportal hepatocytes; α-KG is then partially exported and taken up again by the pericentral hepatocytes, where it is needed for GS [25,26]. After induction of liver damage, the expression of urea cycle enzymes decreased and the pericentral region with GS is completely destroyed. This leads to increased blood ammonia concentrations. However, also GDH is released from damaged hepatocytes and catalyzes a reaction in blood consuming ammonia and α-KG to generate glutamate (Glu). This reaction can go until α-KG in blood is consumed. In this situation α-KG and NADPH should be therapeutically substituted.

Please cite this article in press as: Ghallab A et al. Model-guided identification of a therapeutic strategy to reduce hyperammonemia in liver diseases. J Hepatol (2016), http://dx.doi.org/10.1016/j.jhep.2015.11.018

JOURNAL OF HEPATOLOGY

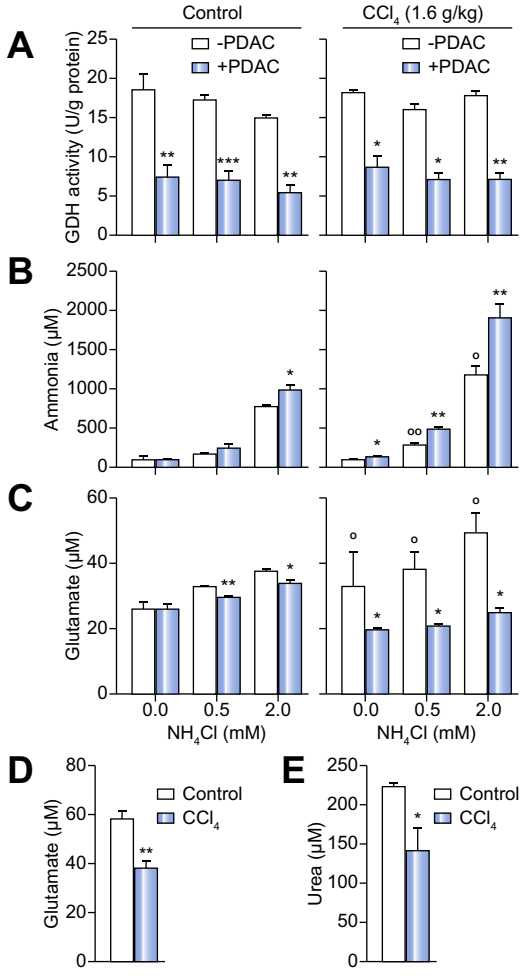

Fig. 4. Ammonia consumption by GDH in primary mouse hepatocytes. Hepatocytes were isolated from CCl_4 (1.6 g/kg) intoxicated (day 1) and untreated mice and suspended at a concentration of 2 million hepatocytes/ml for 1 h with different concentrations of ammonia. (A) Inhibition of GDH activity by PDAC. (B) Compromised ammonia detoxification after GDH inhibition. (C) Reduced glutamate production by GDH inhibition. $^{***}p$ <0.001, $^{**}p$ <0.01 and $^{*}p$ <0.05 compared to – PDAC. $^{\circ\circ}p$ <0.01 and $^{\circ}p$ <0.05 compared to hepatocytes from untreated mice. (D & E) compromised urea and glutamine production by hepatocytes of CCl_4 intoxicated mice. $^{**}p$ <0.01 and $^{*}p$ <0.05 compared to hepatocytes from untreated mice. Data are mean values and SD of three independent experiments.

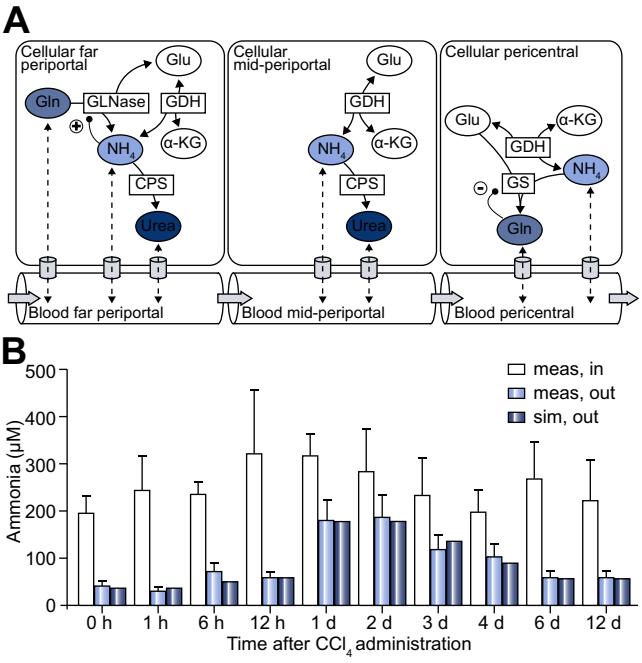

Fig. 5. Integration of the GDH reaction into the metabolic model. (A) Scheme of the metabolic reactions and zones of the extended model including GDH in the blood of the liver and hepatocytes. (B) The model extension leads to a better fit between simulated and experimental data.

In the aforementioned experiment, the molar amount of glutamate produced in the damaged liver after α-KG injection was higher than ammonia consumption (Fig. 6A). Therefore, the results cannot only be explained by the reverse GDH reaction, but may be due to the consumption of α-KG by transaminases that contribute to the generation of glutamate. Indeed, tail vein injection of the transaminases inhibitor AOA prior to α-KG injection reduced the production of glutamate (Fig. 6C) and improved ammonia detoxification. The efficiency of transaminases inhibition by AOA *in vivo* has been confirmed in preliminary experiments (Supplementary Figs. 13 and 14).

The reverse GDH reaction requires NADPH as a cofactor; however, NADPH concentrations are very low in blood. To determine how NADPH levels are altered in our model of liver damage, both NADPH and its oxidized form $NADP^+$ were analyzed. Blood concentrations of both NADPH and $NADP^+$ increased after induction of liver damage by CCl_4 (Supplementary Fig. 15A). In addition, an enhanced $NADP^+$/NADPH ratio was observed in both blood and liver tissue (Supplementary Fig. 15B). This increase in $NADP^+$/NADPH ratio fits to a switch in the GDH reaction from NADPH generation to NADPH consumption. Despite the increase in NADPH after induction of liver damage, the concentrations are still relatively low. Therefore, to study the influence of NADPH, plasma from mice collected 24 h after CCl_4 injection was incubated with varying concentrations of NADPH in the presence of NH_4Cl (1 mM), α-KG (3 mM), AOA (1 mM) and GDH (12,000 U/l) for one hour. A concentration dependent decrease in plasma ammonia and an increase in glutamate were observed with increasing concentrations of NADPH (Fig. 7A). A similar trend for ammonia and glutamate was observed with increasing concentrations of α-KG and GDH (Fig. 7B, C). Moreover, addition of AOA reduced both ammonia and glutamate concentrations (Supplementary Fig. 16). To understand how the orientation of the GDH reaction is controlled by ammonia and glutamate concentrations, titration experiments were performed, which indicated that GDH significantly consumes ammonia beginning at concentrations of 150 μM and higher (Fig. 7D). In contrast, unphysiologically high concentrations of more than 10 mM glutamate were required to block the reaction (Fig. 7E).

Based on these *in vitro* optimized concentrations, we designed an *in vivo* study to treat hyperammonemia in mice. After the induction of liver damage by CCl_4, transaminases activities were inhibited by AOA (13 mg/kg; tail vein injection; 24 h after CCl_4 administration). Thirty minutes later a cocktail of α-KG (280 mg/kg), GDH (720 U/kg) and NADPH (180 mg/kg) was intravenously injected. A dose of 280 mg/kg α-KG was chosen because

Please cite this article in press as: Ghallab A et al. Model-guided identification of a therapeutic strategy to reduce hyperammonemia in liver diseases. J Hepatol (2016), http://dx.doi.org/10.1016/j.jhep.2015.11.018

Research Article

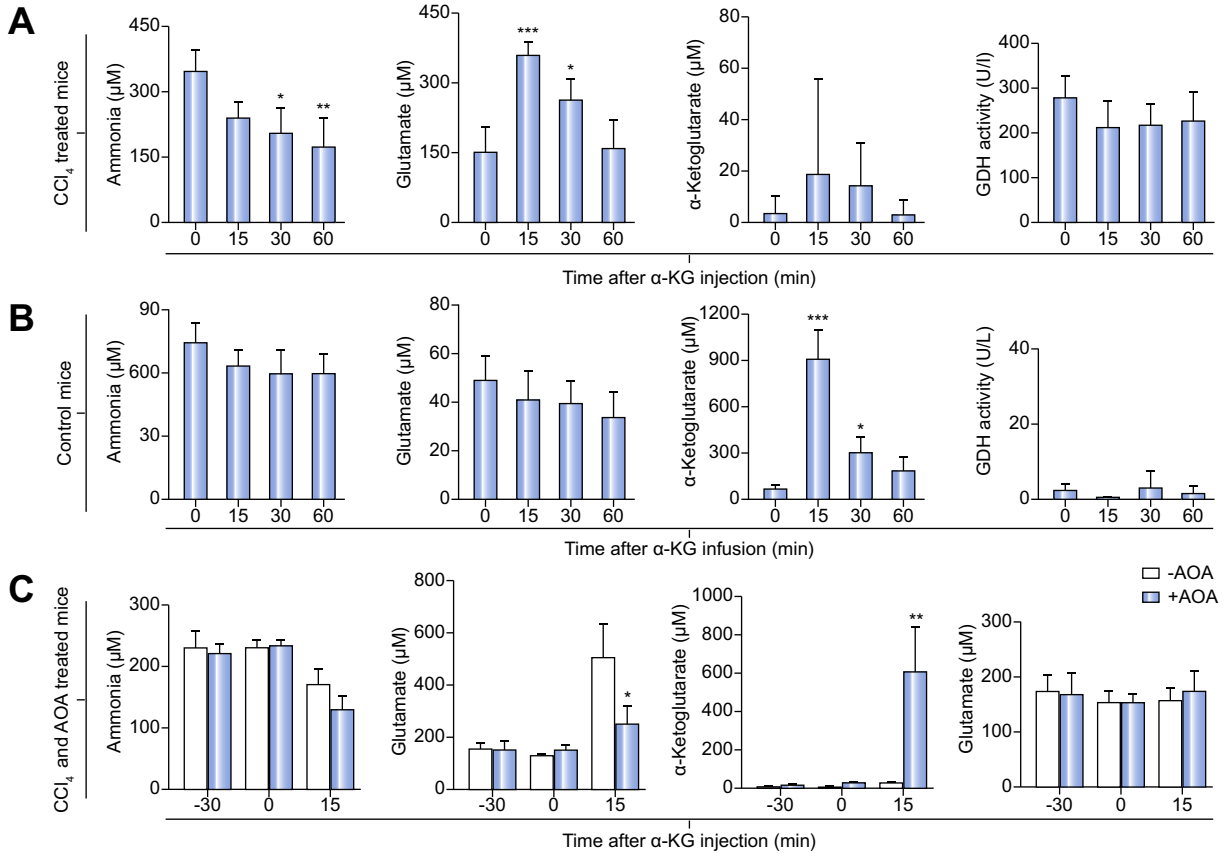

Fig. 6. Reduction of blood ammonia concentrations by α-KG. (A) Tail vein injection of 280 mg/kg α-KG into mice 24 h after induction of liver damage by CCl_4 (1.6 g/kg). (B) Control experiment with α-KG (280 mg/kg) injected into the tail vein of untreated mice. ***p <0.001, **p <0.01 and *p <0.05 when compared to the control group (0). (C) Influence of the transaminase inhibitor, AOA (13 mg/kg; tail vein injection) on ammonia detoxification by α-KG. **p <0.01 and *p <0.05 when compared to the corresponding control. Data are mean values and SD of three mice treated at different experimental days with individually prepared α-KG.

it transiently normalized α-KG levels in mice 24 h after CCl_4. 720 U/kg GDH was used because it resulted in plasma levels of approximately 6000 U/l 15 min after injection (Supplementary Fig. 17), an activity level shown to allow maximal ammonia consumption in plasma *in vitro* (Fig. 7C). The dose of 180 mg/kg NADPH was also considered as adequate in a pharmacokinetic experiment (Supplementary Fig. 18) as it transiently increased plasma NADPH to approximately 1.6 mM 2 min after injection. Injection of the α-KG/GDH/NADPH cocktail (KGN cocktail) reduced ammonia concentrations from 213 to 74 μM within 15 min after administration (Fig. 8). Simultaneously, glutamate levels increased from 131 to 369 μM. Analysis of α-KG and GDH activity in the plasma showed that substitution was successful 15 min after the injection of the KGN cocktail. Moreover, the activities of aspartate and alanine aminotransferase were successfully inhibited by AOA. The mice were observed for three weeks after the experiment and did not show any complications.

Discussion

Guided by simulations with an IM predicting a missing ammonia sink after severe CCl_4-induced liver damage, we identified the GDH reaction as fundamental for ammonia consumption, which can be used therapeutically by the administration of a cocktail of GDH and cofactors.

Therapy for hyperammonemia remains challenging [8–10]. Hemodialysis is the most efficient treatment for reducing elevated blood ammonia concentrations [11,12]. For milder forms of hyperammonemia, pharmacologic management is possible [13]. Efficient strategies for patients with urea cycle defects include infusion of phenylacetate or benzoate. Phenylacetate combines with glutamine to form a product which can be excreted by the kidneys [9,13,14]. Conversely, benzoate combines with glycine to form hippurate, which is also excreted in urine [13,15]. Both compounds reduce the total body nitrogen content; however, this therapy has also failed in a fraction of patients with hyperammonemic crisis who became refractory most probably due to the accumulation of nitrogen waste [9]. This led to the concept that only blood ammonia concentrations below 500 μM should be treated pharmacologically; whereas, more severe hyperammonemia requires aggressive interventions with renal replacement therapies, such as hemodialysis [12,16]. In such situations with either severe or refractory hyperammonemia the therapeutic strategy developed in the present study may be an alternative to hemodialysis.

The current experiments demonstrate that infusion of a KGN-cocktail reduces ammonia close to normal levels within minutes.

Please cite this article in press as: Ghallab A et al. Model-guided identification of a therapeutic strategy to reduce hyperammonemia in liver diseases. J Hepatol (2016), http://dx.doi.org/10.1016/j.jhep.2015.11.018

JOURNAL OF HEPATOLOGY

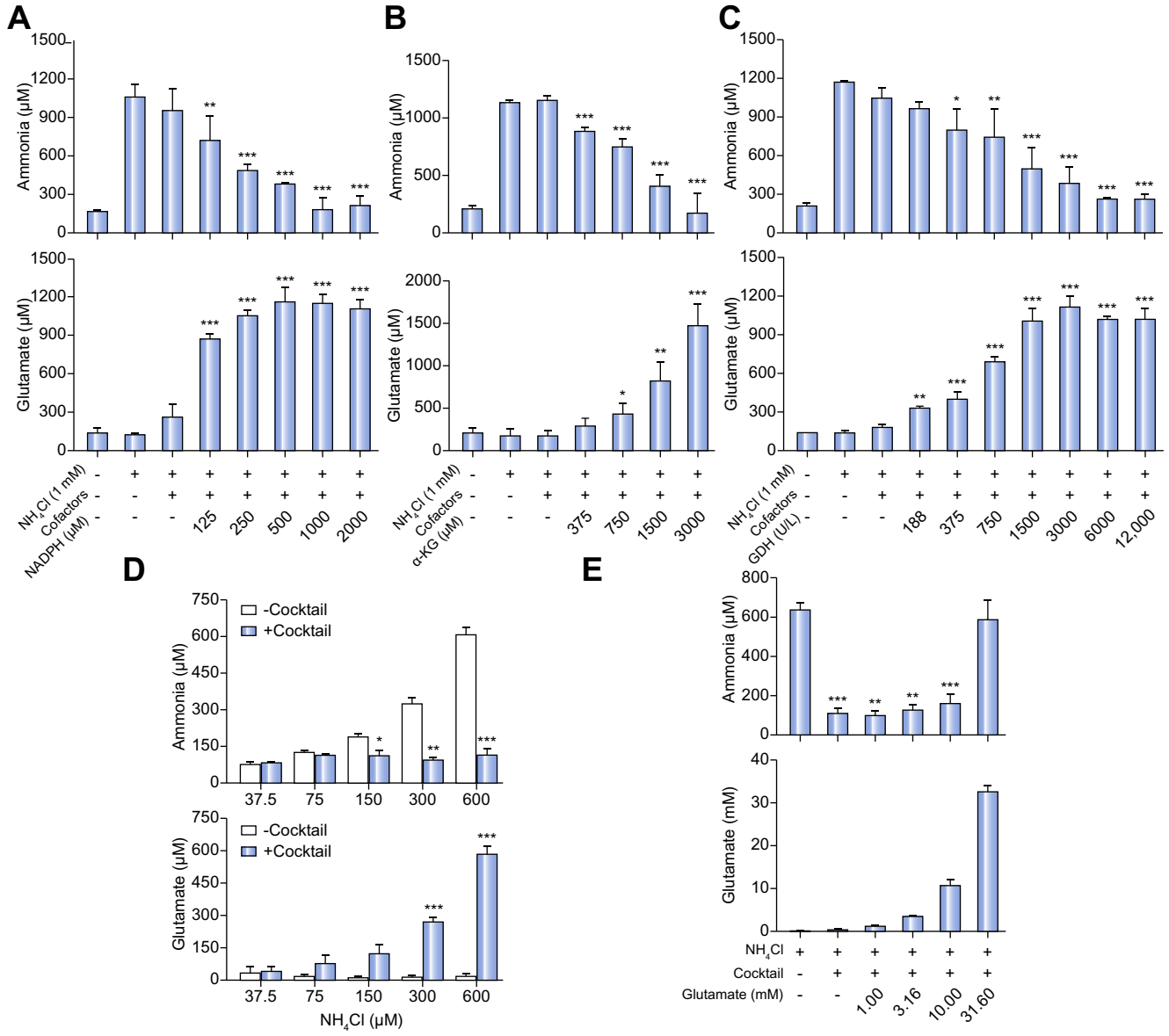

Fig. 7. Optimization of cofactor concentrations for the GDH reaction and identification of maximal GDH activity. (A) NADPH: mouse plasma collected 24 h after CCl_4 injection was incubated with varying concentrations of NADPH in the presence of NH_4Cl (1 mM) and other cofactors; aminooxy acetate (AOA) (1 mM), α-KG (3 mM) and GDH (12,000 U/L) for one hour. (B) Alpha-ketoglutarate (α-KG): plasma was collected from mice on day one after CCl_4 administration and incubated with varying concentrations of α-KG in the presence of NH_4Cl (1 mM) and other cofactors; AOA (1 mM), NADPH (1 mM) and GDH (12,000 U/L). (C) GDH: plasma from mice collected 24 h after CCl_4 injection was incubated with varying concentrations of GDH in the presence of NH_4Cl (1 mM) and other cofactors; AOA (1 mM), α-KG (3 mM), and NADPH (1 mM) for one hour. $^{***}p$ <0.001, $^{**}p$ <0.01 and $^{*}p$ <0.05 compared to the situation where the plasma was incubated with only NH_4Cl. (D) Ammonia detoxification by the cocktail. Different ammonia concentrations were added to plasma of untreated mice and a cocktail of α-KG (3 mM), NADPH (0.5 mM), GDH (6000 U/L) and AOA (1 mM) was added to analyze ammonia and glutamate one hour later. $^{***}p$ <0.001, $^{**}p$ <0.01 and $^{*}p$ <0.05 compared – cocktail. (E) Ammonia (600 μM) detoxification by the cocktail was only blocked by unphysiologically high glutamate concentrations. $^{***}p$ <0.001 compared to NH_4Cl alone. Data are mean values and SD of three biological replicas.

Under these conditions, a GDH-catalyzed reaction takes place in blood where ammonia and α-KG are consumed to form glutamate in an NADPH-dependent reaction. GDH was also previously reported to switch its catalytic orientation under physiological conditions. In the periportal compartment of the liver lobule, GDH generates ammonia (Fig. 3D), which fuels the urea cycle. In the pericentral compartment, GDH is known to consume ammonia to generate glutamate for the GS reaction [17–19]. The present study shows by use of a GDH inhibitor that GDH released from damaged liver tissue may catalyze an ammonia consuming reaction under conditions of hyperammonemia. By releasing GDH from damaged hepatocytes into the blood, the damaged liver provides a mechanism that reduces blood ammonia levels. However, this protective mechanism is limited by the availability of the GDH substrate, α-KG. The present study shows that α-KG strongly decreases upon induction of acute liver dam-

Please cite this article in press as: Ghallab A et al. Model-guided identification of a therapeutic strategy to reduce hyperammonemia in liver diseases. J Hepatol (2016), http://dx.doi.org/10.1016/j.jhep.2015.11.018

Research Article

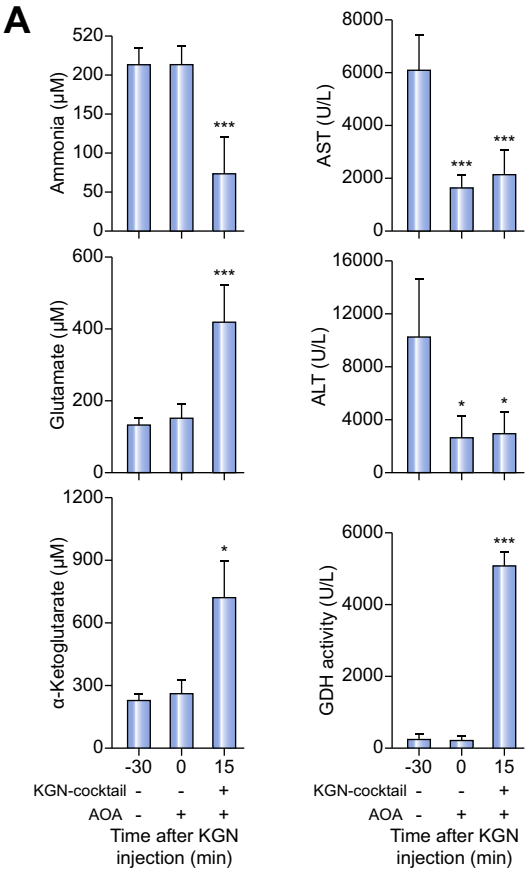

Fig. 8. Treatment of hyperammonemia by injection of a cocktail of GDH and optimized cofactor doses. A cocktail of GDH (720 U/kg), α-KG (280 mg/kg) and NADPH (180 mg/kg) (KGN) was injected into mice 24 h after induction of liver damage using CCl_4 (1.6 g/kg). Thirty minutes prior to treatment with the cocktail, mice received a single dose of 13 mg/kg AOA to block transaminases. Injection of the KGN cocktail reduced ammonia and increased glutamate concentrations in the blood of mice. α-KG and GDH activity increased while aspartate (AST) and alanine aminotransferase (ALT) activities decreased. Data are mean values and SD of four mice treated at different experimental days with individually prepared therapeutic cocktails. $^{***}p$ <0.001, $^{**}p$ <0.01 and $^{*}p$ <0.05 when compared to the control group (−30).

age, because it is consumed by the reverse GDH reaction. This prompted us to supplement α-KG, increase blood concentrations of NADPH, and infuse GDH. Indeed, the combined injection of α-KG, GDH and NADPH efficiently reduced blood ammonia concentrations. A GDH bolus was injected to result in plasma peak concentrations between 5000 and 6000 U/L. This is in the same order of magnitude as observed in patients after acetaminophen intoxication [20]. Therefore, in patients with acute liver intoxication with high blood GDH, therapy with α-KG and NADPH might be sufficient. However, it should be considered that the GDH reaction in blood described here (Fig. 3D) does not explain all experimental observations: α-KG decreases significantly 12 h after CCl_4 administration when there is no significant increase in blood GDH (Fig. 3A). This discrepancy may be explained by the intracellular change of the catalytic direction of GDH in the periportal hepatocytes, which may precede the GDH release into the blood. However, this was not further analyzed in the present study as we choose to focus on the therapeutically more relevant GDH reaction taking place in blood.

α-KG was previously tested for the treatment of hyperammonemia between 1964 and 1978 [21,22], but this strategy was abandoned because it was not sufficiently efficient for clinical application. The reverse GDH reaction in the blood and its requirement for NADPH as a cofactor was not yet known when the early therapeutic studies with α-KG were performed. In addition, injection of α-KG alone in the present study resulted in only a relatively weak reduction of hyperammonemia. This reduction may be possible because in addition to GDH, NADPH is also released from deteriorating hepatocytes after CCl_4 injection.

The concept of treating hyperammonemia by α-KG/GDH/NADPH infusion originates from simulations using an integrated metabolic spatio-temporal model [4]. This model is based on well-understood pathways of ammonia detoxification, such as urea cycle enzymes and the GS reaction [23,24]. It predicted higher ammonia concentrations compared to the measured data. Therefore, we analyzed liver tissue during the damage induction and regeneration processes, but the results could also not explain the discrepancy. Time-resolved gene array experiments following CCl_4 injection led to the observation that a general decrease in metabolizing enzymes occurs including enzymes involved in ammonia metabolism. All enzymes of the urea cycle were transcriptionally downregulated by at least 60%. Factors identified by the gene array analysis were further analyzed by activity assays and immunostaining. Key observations were: (a) the GS positive region, which is initially completely destroyed by CCl_4, shows a delayed recovery and does not return to normal levels before day 12; and (b) CPS1, the rate limiting enzyme in the urea cycle normally expressed in the periportal region, is downregulated during the destruction process (days 1–3), but its expression then extends throughout the entire liver lobule during days 4–6. The other urea cycle enzymes showed a similar time course as CPS1 with the exception of arginase1, which decreased only slightly during the destruction and regeneration process. Glutaminase showed a similar time course and pattern as CPS1. Nevertheless, none of these alterations could explain the observed discrepancy. However, the refined models that take into account the reversible GDH reaction show an excellent agreement with the experimental data suggesting that consumption by the GDH reaction represents the previously predicted ammonia sink, hence providing an example for model guided experimentation.

In conclusion, a novel form of therapy has been identified that allows the rapid correction of hyperammonemia by the infusion of α-KG, GDH and NADPH. This pharmacotherapy may prove relevant as an emergency therapy for episodes of hyperammonemia in urea cycle disease or liver cirrhosis.

Financial support

This study was supported by the BMBF funded projects Virtual Liver (FKZ0315739), Lebersimulator and FP 7EU NOTOX.

Conflict of interest

The authors who have taken part in this study declared that they do not have anything to disclose regarding funding or conflict of interest with respect to this manuscript.

Please cite this article in press as: Ghallab A et al. Model-guided identification of a therapeutic strategy to reduce hyperammonemia in liver diseases. J Hepatol (2016), http://dx.doi.org/10.1016/j.jhep.2015.11.018

JOURNAL OF HEPATOLOGY

Authors' contributions

Ahmed Ghallab: study concept and design; acquisition of data; analysis and interpretation of data; drafting of the manuscript; statistical analysis; critical revision of the manuscript.
Sebastian G. Henkel: mathematical modeling (integrated model of Schliess *et al.* (2014), model 0 and extrahepatic mass balance); analysis and interpretation of data; drafting of the manuscript
Géraldine Cellière: mathematical modeling (novel ammonia detoxification models, extension of model 0); analysis and interpretation of data; drafting of the manuscript, statistical analysis.
Dominik Driesch: mathematical modeling (integrated model of Schliess *et al.* (2014), model 0 and extrahepatic mass balance); analysis and interpretation of data; drafting of the manuscript.
Stefan Hoehme: mathematical modeling (integrated model of Schliess *et al.* (2014), model 0); analysis and interpretation of data; drafting of the manuscript.
Ute Hofmann: acquisition of data; analysis and interpretation of data; technical support; drafting of the manuscript.
Sebastian Zellmer: study concept and design; acquisition of data; analysis and interpretation of data; drafting of the manuscript; critical revision of the manuscript.
Patricio Godoy: acquisition of data; analysis and interpretation of data; drafting of the manuscript.
Agapios Sachinidis: acquisition of data; analysis and interpretation of data; drafting of the manuscript.
Meinolf Blaszkewicz: acquisition of data; analysis and interpretation of data; technical support; drafting of the manuscript.
Raymond Reif: analysis and interpretation of data; drafting of the manuscript.
Rosemarie Marchan: critical revision of the manuscript.
Lars Kuepfer: mathematical modeling; drafting of the manuscript.
Dieter Häussinger: study concept and design; critical revision of the manuscript.
Dirk Drasdo: study concept and design; mathematical modeling (integrated model of Schliess *et al.* (2014), model 0 and novel models); analysis and interpretation of data; drafting of the manuscript, statistical analysis, critical revision of the manuscript
Rolf Gebhardt: study concept and design; acquisition of data; analysis and interpretation of data; drafting of the manuscript, critical revision of the manuscript.
Jan G. Hengstler: study concept and design; acquisition of data; analysis and interpretation of data; drafting of the manuscript, statistical analysis, critical revision of the manuscript; study supervision.

Acknowledgments

We thank Mrs. Gabi Baumhoer, Mrs. Georgia Günther and Mrs. Brigitte Begher-Tibbe – Leibniz Research Centre for Working Environment and Human Factors at the Technical University Dortmund, Dortmund, Germany; and Ms. Margit Henry and Ms. Tamara Rotshteyn – Institute of Neurophysiology and Center for Molecular Medicine Cologne (CMMC), University of Cologne, Cologne, Germany – for competent technical assistance.

Supplementary data

Supplementary data associated with this article can be found, in the online version, at http://dx.doi.org/10.1016/j.jhep.2015.11.018.

References

Author names in bold designate shared co-first authorship

[1] Drasdo D, Hoehme S, Hengstler JG. How predictive quantitative modelling of tissue organisation can inform liver disease pathogenesis. J Hepatol 2014;61:951–956.
[2] **Zellmer S**, **Schmidt-Heck W**, **Godoy P**, **Weng H**, Meyer C, Lehmann T, et al. Transcription factors ETF, E2F, and SP-1 are involved in cytokine-independent proliferation of murine hepatocytes. Hepatology 2010;52:2127–2136.
[3] **Godoy P**, **Hewitt NJ**, Albrecht U, Andersen ME, Ansari N, Bhattacharya S, et al. Recent advances in 2D and 3D in vitro systems using primary hepatocytes, alternative hepatocyte sources and non-parenchymal liver cells and their use in investigating mechanisms of hepatotoxicity, cell signaling and ADME. Arch Toxicol 2013;87:1315–1530.
[4] **Schliess F**, **Hoehme S**, **Henkel SG**, **Ghallab A**, Driesch D, Bottger J, et al. Integrated metabolic spatial-temporal model for the prediction of ammonia detoxification during liver damage and regeneration. Hepatology 2014;60:2040–2051.
[5] **Hoehme S**, **Brulport M**, Bauer A, Bedawy E, Schormann W, Hermes M, et al. Prediction and validation of cell alignment along microvessels as order principle to restore tissue architecture in liver regeneration. Proc Natl Acad Sci U S A 2010;107:10371–10376.
[6] Campos G, Schmidt-Heck W, Ghallab A, Rochlitz K, Putter L, Medinas DB, et al. The transcription factor CHOP, a central component of the transcriptional regulatory network induced upon CCl4 intoxication in mouse liver, is not a critical mediator of hepatotoxicity. Arch Toxicol 2014;88:1267–1280.
[7] Gebhardt R, Baldysiak-Figiel A, Krugel V, Ueberham E, Gaunitz F. Hepatocellular expression of glutamine synthetase: an indicator of morphogen actions as master regulators of zonation in adult liver. Prog Histochem Cytochem 2007;41:201–266.
[8] Levesque R, Leblanc M, Cardinal J, Teitlebaum J, Skrobik Y, Lebrun M. Haemodialysis for severe hyperammonaemic coma complicating urinary diversions. Nephrol Dial Transplant 1999;14:458–461.
[9] Enns GM, Berry SA, Berry GT, Rhead WJ, Brusilow SW, Hamosh A. Survival after treatment with phenylacetate and benzoate for urea-cycle disorders. N Engl J Med 2007;356:2282–2292.
[10] Poh Z, Chang PE. A current review of the diagnostic and treatment strategies of hepatic encephalopathy. Int J Hepatol 2012;2012 480309.
[11] Clay AS, Hainline BE. Hyperammonemia in the ICU. Chest 2007;132:1368–1378.
[12] Rajpoot DK, Gargus JJ. Acute hemodialysis for hyperammonemia in small neonates. Pediatr Nephrol 2004;19:390–395.
[13] Summar M. Current strategies for the management of neonatal urea cycle disorders. J Pediatrics 2001;138:S30–S39.
[14] Honda S, Yamamoto K, Sekizuka M, Oshima Y, Nagai K, Hashimoto G, et al. Successful treatment of severe hyperammonemia using sodium phenylacetate powder prepared in hospital pharmacy. Biol Pharm Bull 2002;25:1244–1246.
[15] Misel ML, Gish RG, Patton H, Mendler M. Sodium benzoate for treatment of hepatic encephalopathy. Gastroenterol Hepatol 2013;9:219–227.
[16] Collen JF, Das NP, Koff JM, Neff RT, Abbott KC. Hemodialysis for hyperammonemia associated with ornithine transcarbamylase deficiency. Appl Clin Genet 2008;1:1–5.
[17] Boon L, Geerts WJ, Jonker A, Lamers WH, Van Noorden CJ. High protein diet induces pericentral glutamate dehydrogenase and ornithine aminotransferase to provide sufficient glutamate for pericentral detoxification of ammonia in rat liver lobules. Histochem Cell Biol 1999;111:445–452.

Please cite this article in press as: Ghallab A et al. Model-guided identification of a therapeutic strategy to reduce hyperammonemia in liver diseases. J Hepatol (2016), http://dx.doi.org/10.1016/j.jhep.2015.11.018

Research Article

[18] Sies H, Häussinger D, Grosskopf M. Mitochondrial nicotinamide nucleotide systems: ammonium chloride responses and associated metabolic transitions in hemoglobin-free perfused rat liver. Hoppe Seylers Z Physiol Chem 1974;355:305–320.
[19] Spanaki C, Plaitakis A. The role of glutamate dehydrogenase in mammalian ammonia metabolism. Neurotox Res 2012;21:117–127.
[20] McGill MR, Sharpe MR, Williams CD, Taha M, Curry SC, Jaeschke H. The mechanism underlying acetaminophen-induced hepatotoxicity in humans and mice involves mitochondrial damage and nuclear DNA fragmentation. J Clin Invest 2012;122:1574–1583.
[21] Meuret G, Beck K, Keul J, Gruenagel HH. On therapy of hepatic coma with metabolites of the urea cycle, glutamate and alpha-ketoglutarate. Dtsch Med Wochenschr 1968;93:1194–1197.
[22] Wildhirt E. The terminal stage of liver diseases and hepatic coma. Der Internist 1965;6:439–446.
[23] Gebhardt R, Mecke D. Heterogeneous distribution of glutamine synthetase among rat liver parenchymal cells in situ and in primary culture. EMBO J 1983;2:567–570.
[24] Häussinger D. Hepatocyte heterogeneity in glutamine and ammonia metabolism and the role of an intercellular glutamine cycle during ureogenesis in perfused rat liver. Eur J Biochem 1983;133:269–275.
[25] Stoll B, Häussinger D. Hepatocyte heterogeneity in uptake and metabolism of malate and related dicarboxylates in perfused rat liver. Eur J Biochem 1991;195:121–129.
[26] Stoll B, McNelly S, Buscher HP, Häussinger D. Functional hepatocyte heterogeneity in glutamate, aspartate and alpha-ketoglutarate uptake: a histoautoradiographical study. Hepatology 1991;13:247–253.

Please cite this article in press as: Ghallab A et al. Model-guided identification of a therapeutic strategy to reduce hyperammonemia in liver diseases. J Hepatol (2016), http://dx.doi.org/10.1016/j.jhep.2015.11.018